PERGAMON

Available online at www.sciencedirect.com

SCIENCE DIRECT

Polyhedron 22 (2003) 665–671

POLYHEDRON

www.elsevier.com/locate/poly

A new bis(phenol-armed) pyridazine-containing Schiff base ligand: synthesis, complexation and reduction to the amine ligand analogue

Sally Brooker *, Simon S. Iremonger, Paul G. Plieger

Department of Chemistry, University of Otago, P.O. Box 56, Dunedin, New Zealand

Received 31 July 2002; accepted 12 September 2002

Abstract

A bis(phenol-armed) acyclic Schiff base ligand H_2L has been synthesised from 3,6-diformylpyridazine and two equivalents of *o*-aminophenol. The H_2L ligand has been structurally characterised and is shown to be close to planar (maximum twist of pyridazine ring vs. phenyl ring planes is just 17.7°) with both intramolecular and intermolecular hydrogen-bonding interactions present. The latter hydrogen-bonding interactions in combination with offset parallel $\pi-\pi$ stacking interactions are instrumental in the formation of columns of a stepped criss-cross type array. The ligand undergoes an irreversible oxidation in dimethylformamide at $E_{pa} = +0.91$ V vs. 0.01 mol l^{-1} $AgNO_3/Ag_{(s)}$, to form an unstable new compound which exhibits closely spaced quasi-reversible processes at $E_{1/2} \approx -0.77$ V. In addition, there is a process at -0.25 V which is associated with an irreversible reduction process at $E_{pc} = -1.52$ V. Chemical reduction of the two imine bonds of H_2L was achieved by reaction with $NaBH_4$ to give the diamine analogue H_6L' as the dihydrochloride salt: no evidence of pyridazine ring reduction was observed. Three complexes of L^{2-}, $Co_2L(CH_3COO)_2$, $Ni_2L(CH_3COO)_2(H_2O)$ and $Cu_2L(CH_3COO)_2(H_2O)_2(CH_3CN)$, have been prepared and partially characterised.

© 2002 Elsevier Science Ltd. All rights reserved.

Keywords: Pyridazine; Quasi-reversible; Schiff base; *o*-aminophenol

---

1. Introduction

Our interests lie in the development and exploration of families of di- and poly-nuclear transition metal complexes in which heteroaromatic bridging moieties are present. To this end we have used 3,6-diformylpyridazine as a suitable ligand precursor and established the relative ease with which the resulting pyridazine bridging moiety can be incorporated into both *macrocyclic* and *grid* complexes [1–5].

Prior to this work other groups, most notably Thompson et al., utilised *acyclic* pyridazine-containing ligands to bridge a range of transition metal ions, to great effect [5–18]. Thompson et al. have looked in detail at the coordination chemistry, of copper in particular, of a wide range of acyclic pyridazine- and closely related phthalazine-containing ligands [7]. These structural, magnetic and electrochemical studies followed on from earlier work by Blake et al., who were the first to look at the magnetic exchange between metal ions bridged by pyridazine- and phthalazine-containing ligands [8].

Usually the 1,2-diazine moiety in these acyclic pyridazine/phthalazine ligands bridges the two metal ions thereby placing them in close proximity to one another. Often they are also bridged by other groups such as hydroxide [9], halogen [10], sulfate [11], nitrate [12], iodate [13], or azide [14]. The resulting complexes have a range of interesting properties. For example these diazines, particularly pyridazine, are capable of mediating strong anti-ferromagnetic exchange [15] between the metal ions and tend to stabilise low oxidation states [5].

To date, there are relatively few examples of pyridazine or phthalazine cyclic [16] or acyclic [17,18] complexes that also contain a phenol donor, and of these only one example has been structurally characterised [18]. Described here is the synthesis and characterisation of a new acyclic Schiff base ligand, H_2L, and the reduced form, H_6L', both of which incorporate pyridazine and phenol donors (Fig. 1). The resulting cobal-

---

* Corresponding author. Tel.: +64-3-479-7919; fax: +64-3-479-7906.

E-mail address: sbrooker@alkali.otago.ac.nz (S. Brooker).

0277-5387/02/$ - see front matter © 2002 Elsevier Science Ltd. All rights reserved.

doi:10.1016/S0277-5387(02)01398-0

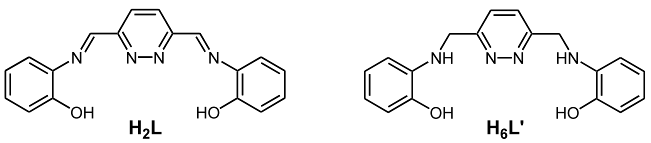

Fig. 1. The ligands synthesised in this study.

t(II), nickel(II) and copper(II) complexes of the ligand L^{2-} are also presented.

2. Experimental

2.1. Starting materials and reaction procedures

As reported previously [1,3] except for the following. 3,6-Diformylpyridazine was synthesised according to the published procedure [3]. *o*-Aminophenol was purchased from the Riedel-de Haen AG Chemical Company and used without further purification. DMF was dried according to the standard procedure [19].

2.2. H_2L (**1**)

3,6-Diformylpyridazine (0.604 g, 4.44 mmol) and *o*-aminophenol (0.969 g, 8.88 mmol) were stirred for 10 min in acetonitrile (60 ml), then allowed to stand for 5 h. The resulting bright yellow crystals were filtered off and washed with ice cold acetonitrile (10 ml). On standing the filtrate overnight, a second crop was obtained (1.126 g, 80%). m.p. 175 °C (dec). (*Anal.* Found: C, 67.8; H, 4.3; N, 17.9. Calc. for $C_{18}H_{14}O_2N_4$: C, 67.9; H, 4.4; N, 17.6%. IR (KBr disk) ν_{max} cm^{-1} 3408, 3376, 1620, 1583, 1352, 802, 766. δ_H (300 MHz, d_7-DMF, ref DMF) 9.55 (2H, s, O*H*), 9.23 (2H, s), 8.82 (2H, s), 7.60 (2H, dd), 7.27 (2H, dt), 7.04 (2H, dd), 6.96 (2H, dt). δ_C (75 MHz, d_7-DMF, ref DMF) 159.0, 156.7, 153.7, 136.8, 130.4, 125.7, 120.5, 120.1, 117.3. FAB *m*/*z* fragment: 319 H_2L^+. UV–Vis (DMF) $\lambda_{max} = 395$ nm, $\varepsilon = 6334$ $l\ mol^{-1}\ cm^{-1}$; $\lambda_{max} = 556$ nm, $\varepsilon = 98$ $l\ mol^{-1}\ cm^{-1}$.

2.3. $H_6L' \cdot 2HCl$ (**2**)

To a stirred room temperature suspension of H_2L (0.160 g, 0.50 mmol) in acetonitrile (40 ml) was added solid sodium borohydride (0.038 g, 1.0 mmol) in small portions over 1 h. The resulting dark red mixture was stirred for 10 min., then brought to reflux for 5 min. On cooling to room temperature the deep red solution was acidified with hydrochloric acid (1.2 M, ≈ 2.5 cm^3) until pH 1. The resulting fine white precipitate was filtered, washed with acetonitrile (2×10 cm^3) and dried in vacuo (0.184 g, 92%, but impure: contaminated with salt). m.p. > 240 °C. IR (KBr disk) ν_{max} cm^{-1} 2673, 2560, 1601, 1577, 1350, 749. δ_H (300 MHz, D_2O, ref DSS) 7.66 (2H, s), 7.20 (2H, t), 7.03 (2H, d), 6.91 (2H, d), 6.81 (2H, t), 4.86 (4H, s). δ_C (300 MHz, D_2O, ref DSS) 157.7, 151.9, 133.0, 132.4, 125.6, 124.9, 123.4, 119.4, 53.9.

2.4. $Co_2L(CH_3COO)_2$ (**3**)

To a yellow suspension of H_2L (0.051 g, 0.16 mmol) in acetonitrile (30 ml), was added $Co(CH_3COO)_2$ (0.057 g, 0.32 mmol) in acetonitrile (10 ml). The resulting deep green mixture was stirred for 48 h, during which time the solution became purple and a purple precipitate formed. This was filtered off, washed with acetonitrile (10 cm^3) and dried in vacuo (0.073 g, 83%). *Anal.* Found: C, 47.6; H, 4.0; N, 10.6. Calc. for $C_{22}H_{18}N_4O_6Co_2$: C, 47.8; H, 3.3; N, 10.2. IR (KBr disk) ν_{max} cm^{-1} 3387, 3052, 1580, 1462, 1414, 1260, 1140, 748. FAB *m*/*z*: 451 $Co_2L(OH)$; 886 $[Co_2L]_2$. UV–Vis (DMF) $\lambda_{max} = 366$ nm, $\varepsilon = 11959$ $l\ mol^{-1}\ cm^{-1}$; $\lambda_{max} = 600$ nm, $\varepsilon = 7231$ $l\ mol^{-1}\ cm^{-1}$. μ (RT) = 3.2 BM per Co.

2.5. $Ni_2L(CH_3COO)_2(H_2O)$ (**4**)

To a yellow suspension of H_2L (0.057 g, 0.18 mmol) in acetonitrile (30 ml), was added $Ni(CH_3COO)_2 \cdot 4H_2O$ (0.080 g, 0.36 mmol) in acetonitrile (30 ml). The resulting deep purple mixture was stirred overnight over which time an intense purple precipitate formed. This was filtered off, washed with acetonitrile (10 ml) and dried in vacuo (0.090 g, 91%). *Anal.* Found: C, 46.6; H, 3.9; N, 10.2. Calc. for $C_{22}H_{18}N_4O_6Ni_2 \cdot H_2O$: C, 46.4; H, 3.5; N, 9.8. IR (KBr disk) ν_{max} cm^{-1} 3388, 3031, 1587, 1456, 1416, 1286, 1142, 749. FAB *m*/*z*: 449 $Ni_2L(OH)$; 882 $[Ni_2L]_2$. UV–Vis (DMF) $\lambda_{max} = 366$ nm, $\varepsilon = 13474$ $l\ mol^{-1}\ cm^{-1}$; $\lambda_{max} = 580$ nm, $\varepsilon = 9962$ $l\ mol^{-1}\ cm^{-1}$. μ (RT) = 2.8 BM per Ni.

2.6. $Cu_2L(CH_3COO)_2(H_2O)_2CH_3CN$ (**5**)

To a yellow suspension of H_2L (0.067 g, 0.21 mmol) in acetonitrile (40 ml), was added $Cu(CH_3COO)_2 \cdot H_2O$ (0.084 g, 0.42 mmol) in acetonitrile (15 ml). The resulting deep purple mixture was stirred overnight. An intense blue precipitate formed, which was filtered off, washed with acetonitrile (10 ml) and dried in vacuo (0.082 g, 69%). *Anal.* Found: C, 45.3; H, 3.8; N, 10.9. Calc. for $C_{22}H_{18}N_4O_6Cu_2 \cdot 2H_2O \cdot CH_3CN$: C, 45.1; H, 3.8; N, 11.0. IR (KBr disk) ν_{max} cm^{-1} 3441, 2924, 1605, 1576, 1512, 1444, 1414, 1282, 1131, 745. FAB *m*/*z*: 886 $[Cu_2L]_2$; 596 $Cu_2L(CH_3COO)_2(H_2O)_2$; 578 $Cu_2L(CH_3COO)_2(H_2O)$; 536 $Cu_2L(CH_3COO)$; 461 $Cu_2L(H_2O)$; 443 Cu_2L. UV–Vis (DMF) $\lambda_{max} = 314$ nm, $\varepsilon = 10843$ $l\ mol^{-1}\ cm^{-1}$; $\lambda_{max} = 352$ nm, $\varepsilon = 12014$ $l\ mol^{-1}\ cm^{-1}$; $\lambda_{max} = 528$ nm, $\varepsilon = 10216$ $l\ mol^{-1}\ cm^{-1}$). μ (RT) = 1.3 BM per Cu.

3. X-ray crystallography

X-ray data were collected at 168 K on a Bruker SMART diffractometer using graphite-monochromated Mo Kα radiation and used after a semi-empirical absorption correction had been applied. The structure was solved using SHELXS-97 [20] and refined against all F^2 data using SHELXS-97 [21].

3.1. Crystal data for H_2L (*1*)

$C_{18}H_{14}N_4O_2$, yellow plate, $0.50 \times 0.30 \times 0.10$ mm, orthorhombic, *Pbca*, $a = 11.481(5)$, $b = 9.349(5)$, $c = 28.845(14)$ Å, $U = 3096(3)$ Å^3, $T = 168(2)$ K, $Z = 8$, $\mu = 0.093$ mm^{-1}. 12 242 Reflections collected in the range $4.64° < 2\theta < 45°$ and the 2011 independent reflections were used in the structural analysis. The structure was solved by direct methods and refined to $R_1 = 0.0541$ [for 1018 $F > 4\sigma(F)$; $\omega R_2 = 0.1349$ and goodness-of-fit $= 0.887$ for all 2011 F^2; 218 parameters; all non-hydrogen atoms anisotropic].

4. Results and discussion

4.1. Synthesis of free ligand H_2L (*1*)

The free ligand **1** was readily made from the reaction of 3,6-diformylpyridazine with *o*-aminophenol in acetonitrile solution. Upon standing, small thin bright yellow plates precipitated in good yield over a number of hours.

The IR spectrum of **1** exhibits a sharp C=N stretch at 1620 cm^{-1} and no evidence of either primary amine stretches or of a carbonyl stretch. The phenol O–H stretch is present, and is split (3408 and 3376 cm^{-1}) as a consequence of both the intra- and intermolecular hydrogen-bonding present (Figs. 2 and 3). There are bands present for aromatic C–H stretches (3071 and 3052 cm^{-1}) and pyridazine ring stretches (1583 cm^{-1}). The out-of-plane C–H bending absorption for an o-disubstituted aromatic (766 cm^{-1}) is also seen. Due to the poor solubility of **1** the NMR spectra were recorded in deuterated DMF. The FAB mass spectrum of **1** contained the expected parent ion and associated fragmentation pattern. The ligand decomposed at ~175 °C.

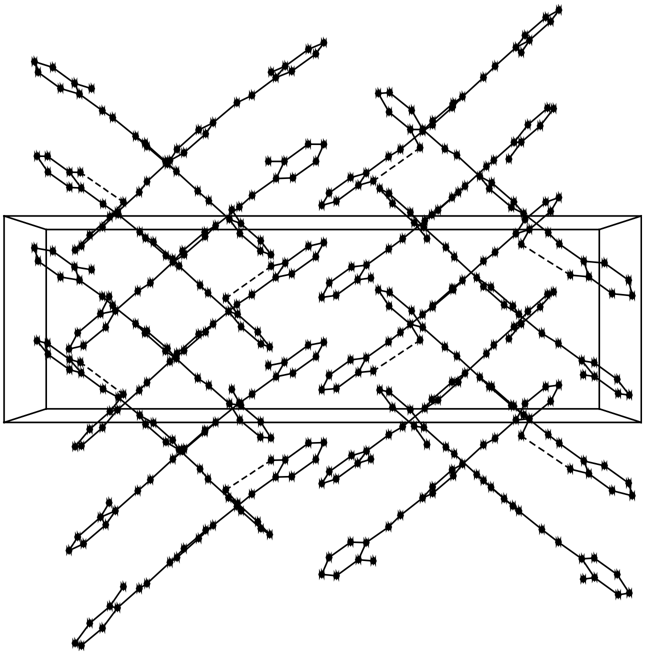

Fig. 3. The packing diagram of compound **1**, viewed down the *a* axis, reveals columns of stepped criss-cross arrays which are stabilised by the combined effects of π–π and hydrogen-bonding interactions.

4.2. Molecular structure of *1*

The molecular structure of **1** is shown in Figs. 2 and 3, and selected bond lengths and angles are listed in Table 1. The first thing of note about the structure of **1** is that the pyridazine ring is rotated ca. 180° away from the imine nitrogen atoms and phenolic protons, that is to say, it adopts an all trans configuration. This conformation has also been observed in the cryptand prepared from 3.6-piformylpyridazine and *tren* [4]. The pyridazine diimine unit is fairly flat [the maximum displacement from the pyridazine ring mean plane is 0.115(7) Å for N(4)], but there is a slight twist between the pyridazine and phenyl ring planes [17.7(2) and 11.1(2)° for the C(8) and C(16) phenyl rings respectively]. Strong intramolecular hydrogen-bonding is present between the phenolic protons (which were located from difference maps) and the imine nitrogen atoms: O(1)–H(1)···N(3) 2.697 Å and O(2)–H(2)···N(4) 2.634 Å.

Each molecule of H_2L shares four intermolecular hydrogen-bonds (two each of 2.904 and 3.037 Å, by

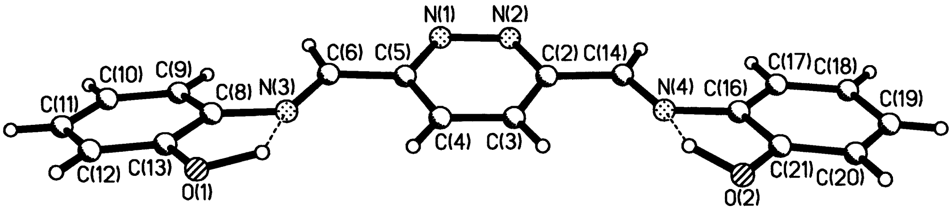

Fig. 2. Perspective view of the free ligand H_2L (**1**), showing the strong intramolecular hydrogen-bonds between the phenol oxygen atoms (O1 and O2) and the imine nitrogen atoms (N3 and N4, respectively).

Table 1
Selected bond lengths (Å) and angles (°) for the ligand H_2L (**1**)

Selected bond lengths		*Selected torsion angles*	
N1–N2	1.339(5)	C4–C5–C6–N3	−1.4(7)
N1–C5	1.344(5)	C6–N3–C8–C9	18.1(7)
N2–C2	1.339(5)	C6–N3–C8–C13	−164.9(4)
C6–N3	1.270(5)	C3–C2–C14–N4	−2.4(6)
N3–C8	1.399(5)	C14–N4–C16–C17	−9.4(7)
C13–O1	1.367(5)		
C14–N4	1.266(5)	*Selected H-bond lengths (intra)*	
N4–C16	1.394(5)	O1–N3	2.697
C21–O2	1.382(5)	O2–N4	2.634
Selected bond angles		*Selected H-bond lengths (inter)*	
N2–N1–C5	120.1(4)	O1–O2	2.904
N1–N2–C2	119.4(4)	O2–N2	3.037
N2–C2–C3	122.2(4)	O2–N1	3.263

symmetry) with four of the perpendicularly orientated nearest neighbours (Fig. 3). Further, the individual molecules of H_2L are stacked up in off-set parallel π–π stacks. The overall result of the combination of these two intermolecular interactions is columns of stepped criss-cross arrays (Fig. 3).

4.3. Electrochemistry of H_2L

Cyclic voltammograms were obtained for H_2L in DMF, at a concentration of 1 mmol l^{-1}, and were referenced to 0.01 mol l^{-1} $AgNO_3$ in $CH_3CN/Ag_{(s)}$. As a further reference check, ferrocene was added at the conclusion of the experiment: the Fc/Fc^+ couple occurred at $E_{1/2} = +0.07 \pm 0.01$ V with $\Delta E = 0.07$ V.

On scanning from −0.60 V to more negative potentials, the cyclic voltammogram for **1** in DMF revealed an irreversible reduction process at $E_{pc} = -1.52$ V (Fig. 4). On reversing the scan direction at −1.80 V, a process associated with this reduction appeared at −0.25 V. This reduction process may be due to the partial reduction of the imine bonds to secondary amines (and subsequent protonation by phenol). In general, the reduction of imines is believed to occur via two well-separated steps and can follow one of two mechanisms [22], with the first one electron reduction commonly occurring anywhere in the range from −1.3 to −1.8 V vs. SCE for conjugated organic compounds in DMF [23]. On scanning to more negative potentials a quasi-reversible reduction process ($E_{1/2} = -2.04$ V, $\Delta E = 0.20$ V), on the edge of the electrochemical window, is also observed. This process may also be associated with the reduction of the imine bonds (Section 4.4), however, it should be noted that the possibility that some or all of these processes may instead be based on the pyridazine ring can not be ruled out [24].

On scanning from 0.0 V to positive potentials there is a multi-electron irreversible oxidation process at $E_{pa} = +0.91$ V (Fig. 5). Further investigation revealed that associated with this process are two (almost identically placed) quasi-reversible processes at $\approx E_{1/2} = -0.77$ V. At slow scan rates only one process is seen, with $\Delta E = 0.10$ V, but on going to higher scan rates (1 V s^{-1}), the processes become more spread and the second process is revealed as a shoulder on the first. This indicates that oxidation of the original H_2L ligand, followed by a chemical rearrangement, generates a new chemical species which exhibits quasi-reversible chemistry. A possible explanation is that upon irreversible oxidation H_2L undergoes an intramolecular rearrangement to form 3,6-dibenzoxazolepyridazine (a common method for the synthesis of benzoxazoles from substituted 2-iminophenols is via oxidation using various mild chemical oxidants) [25]. Also, phenyl substituted benzoxazoles have been shown to stabilise anion π-radicals [26], hence the quasi-reversible processes occurring at $E_{1/2} = -0.77$ V may be associated with this species.

It was not possible to study the electrochemistry of the virtually insoluble complexes of H_2L.

4.4. Synthesis of $H_6L'\cdot 2HCl$ (**2**)

Conversion of the Schiff base ligand H_2L to the diamine analogue H_6L' was conveniently achieved by $NaBH_4$ reduction in acetonitrile solution. Subsequent acidification with hydrochloric acid gave the dihydrochloride salt of H_6L', **2**, as an impure white precipitate in 92% yield. IR, ^1H NMR and ^{13}C NMR analyses were all consistent with the complete conversion of the imine functionalities to secondary amines, with no evidence of pyridazine ring reduction (Section 4.3). The NMR spectra showed that the product was not contaminated by detectable amounts of any organic impurities, however, elemental analysis revealed the presence of an inorganic salt contamination of ≈20% which proved difficult to remove due to the similar solubility of both product and contaminant.

4.5. Complexes of H_2L

The Co(II), Ni(II) and Cu(II) complexes of **1** were conveniently prepared by stirring the appropriate metal acetate salt with **1**, in acetonitrile, over several hours. All three complexes precipitated in good yields as virtually insoluble blue or purple powders. All attempts to grow single crystals from these rather insoluble solids were unsuccessful, as were attempts to grow crystals by slowly diffusing solutions of **1** and the appropriate metal acetate salt together over many weeks.

The IR spectra of these three complexes, in addition to bands due to **1**, contain bands associated with the acetate anions. Two bands are expected for the C–O stretches of the acetate ion, namely the symmetrical (1300–1450 cm^{-1}) and asymmetrical (1500–1750 cm^{-1}) [27] stretches. A correlation exists between the

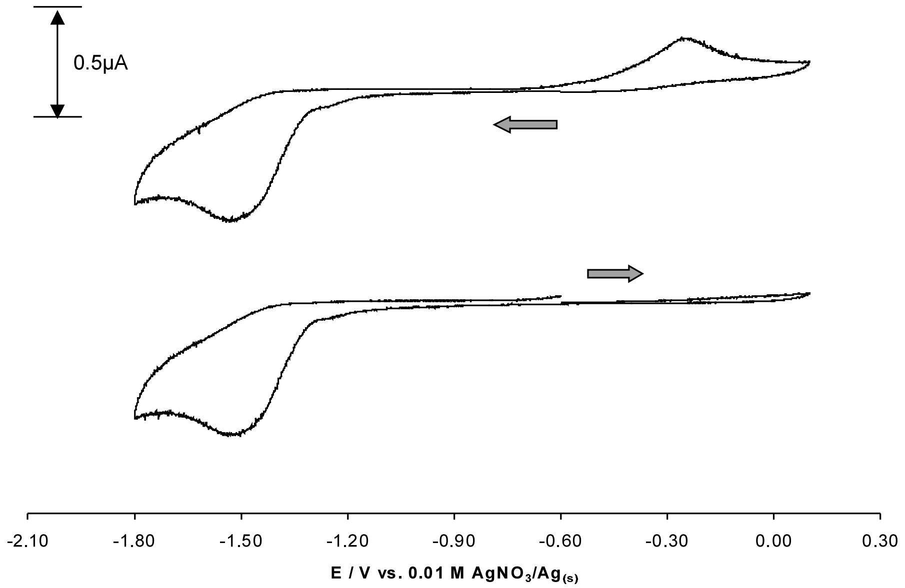

Fig. 4. Cyclic voltammograms of H_2L at 200 mV s^{-1} in DMF. The top cyclic voltammogram was produced by scanning to more negative potentials first. The bottom cyclic voltammogram was generated by scanning to positive potentials first. In both cases $E_I = -0.60$ V.

magnitude of the difference between these stretches (Δ) and the mode of acetate co-ordination [28]. When $\Delta \geqslant 200$ cm^{-1} the acetate is co-ordinated through one oxygen atom (unidentate), when $\Delta \leqslant 150$ cm^{-1} then both oxygen atoms are co-ordinated to the same metal (bidentate chelating) and in the intermediate region ($150 < \Delta < 200$ cm^{-1}) the mode of co-ordination is either bidentate chelating or 1,3-bridging bidentate [28]. Whilst it is difficult to identify these bands unambiguously, tentative assignments lead to Δ values of 167, 176 and 162 cm^{-1} for the cobalt, nickel and copper complexes respectively. These values imply that in all of the complexes the acetate ions are bidentate chelating, 1,3-bridging bidentate or ionic. It is thought that, due to the rigid nature of L^{2-} and the donor requirements of the metal ions, the 1,3-bridging bidentate co-ordination mode may be that which is present in these complexes. Unfortunately the compounds were too insoluble for standard conductivity measurements to be carried out so it was not possible to rule out the ionic acetate option, but this mode seems unlikely especially given the low solubility.

The FAB mass spectra of compounds **3**–**5** all show similar fragmentation patterns. Each spectrum has peaks corresponding to the loss of the acetate anions, and also peaks corresponding to hydrated species, such as M_2LOH, which presumably arise from the damp solvent used to introduce the samples to the mass

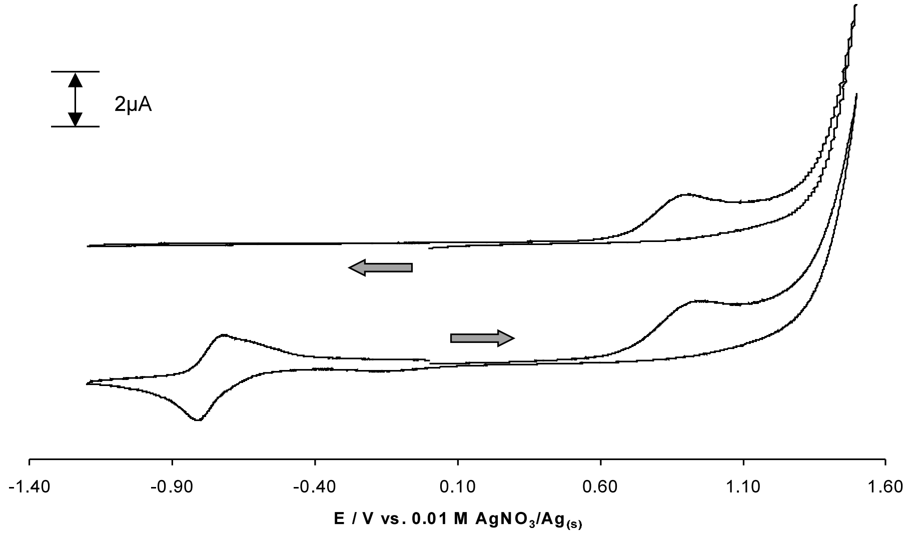

Fig. 5. Cyclic voltammograms of H_2L at 200 mV s^{-1} in DMF. The top cyclic voltammogram was produced by scanning to negative potentials first. The bottom cyclic voltammogram was generated by scanning to positive potentials first. In both cases $E_I = 0.0$ V.

spectrometer. Peaks were also identified for the dimerised fragment $[M_2L]_2$ so a dimeric, or indeed a polymeric, morphology for these complexes cannot be ruled out.

The observed magnetic moment for the nickel complex **4** is close to the expected spin-only value and is typical for a high spin octahedral nickel(II) complex. For the copper and cobalt complexes the observed values of magnetic moment are somewhat lower than the spin-only values expected for isolated copper(II) and high spin cobalt(II) ions (3.88 and 1.73 BM for **3** and **5** respectively). In the absence of structural data for these complexes this has not been pursued further.

Dilute DMF solutions of all three complexes are highly coloured and display intense absorptions in the UV and visible regions. In the region 300–400 nm, charge transfer transitions with intensities exceeding 10 800 $\mathrm{l\,mol^{-1}\,cm^{-1}}$ are observed in all cases and in the visible region intense bands are observed in the range 520–600 nm, which mask any d–d transitions. The $Cu_2L(CH_3COO)_2$ complex has an additional absorbance, over those observed for both the nickel or cobalt complexes, at 314 nm ($\varepsilon = 10\,843$ $\mathrm{l\,mol^{-1}\,cm^{-1}}$). The Mo(V) complex of a structurally similar phthalazine ligand also exhibits a similar electronic spectrum, with bands for the DMF co-ordinated complex observed at 370 nm and 549 nm [18]. The extensive π-conjugation present in these types of ligands clearly facilitates these charge transfer transitions.

Due to the insoluble nature of these complexes further solution studies were not possible.

5. Conclusion

The pyridazine and phenol containing acyclic Schiff base ligand H_2L, and the amine analogue H_6L', have been prepared and characterised. The solid state X-ray structure of H_2L was determined and revealed both intra- and intermolecular hydrogen-bonding as well as intermolecular π–π stacking. These intermolecular interactions resulted in the generation of columns of stepped criss-cross type arrays. The electrochemistry of H_2L in DMF revealed two reduction processes that are probably due to the reduction of the imine functional groups to secondary amines and one oxidation process that resulted in a new species with quasi-reversible electrochemistry. Some metal acetate complexes of L^{2-} were isolated and partially characterised. Unfortunately, due to the low solubility of these complexes, the solution chemistry could not be fully explored. It is suggested that anyone considering future work in this area would need to consider (a) developing synthetic routes to utilise anions other than acetate and/or (b) adding solubilising substituents to the ligand framework, for example by employing a more highly substituted amine component such as 2-amino-4-*tert*-amylphenol which is commercially available.

6. Supplementary data

Supplementary data for the structure of compound **1** are available from the CCDC, 12 Union Road, Cambridge CB2 1EZ, UK (fax: +44-1223-336033; e-mail: deposit@ccdc.cam.ac.uk) on request, quoting the deposition number CCDC 191171.

Acknowledgements

This work was supported by grants from the University of Otago and, more recently, the Marsden Fund (Royal Society of New Zealand). We are grateful to the University of Otago for the award of an Otago Postgraduate Scholarship to P.G.P. We thank Dr J. Wikaira and Professor W.T. Robinson (University of Canterbury) for the X-ray data collection and B.M. Clark for the FAB mass spectra (University of Canterbury).

References

[1] S. Brooker, T.C. Davidson, S.J. Hay, R.J. Kelly, D.K. Kennepohl, P.G. Plieger, B. Moubaraki, K.S. Murray, E. Bill, E. Bothe, Coord. Chem. Rev. 216–217 (2001) 3.

[2] (a) S. Brooker, R.J. Kelly, B. Moubaraki, K.S. Murray, Chem. Commun. (1996) 2579;
(b) S. Brooker, R.J. Kelly, P.G. Plieger, Chem. Commun. (1998) 1079;
(c) S. Brooker, P.G. Plieger, B. Moubaraki, K.S. Murray, Angew. Chem. Int. Ed. 38 (1999) 408 (and front cover);
(d) S. Brooker, S.J. Hay, P.G. Plieger, Angew. Chem. Int. Ed. 39 (2000) 1968;
(e) S. Brooker, R.J. Kelly, G.M. Sheldrick, J. Chem. Soc. Chem. Commun. (1994) 487.

[3] S. Brooker, R.J. Kelly, J. Chem. Soc. Dalton Trans. (1996) 2117.

[4] (a) S. Brooker, J.D. Ewing, J. Nelson Inorg. Chim. Acta 317 (2001) 53;
(b) S. Brooker, J.D. Ewing, J. Nelson, J.C. Jeffery, Inorg. Chim. Acta. 337, (2002) 463.

[5] S. Brooker, Eur. J. Inorg. Chem. (2002) 2535 (and front cover).

[6] (a) N.D. Sung, K.S. Yun, T.Y. Kim, K.Y. Choi, M. Suh, J.G. Kim, I.H. Suh, J. Chin, Inorg. Chem. Commun. 4 (2001) 377;
(b) K.Y. Choi, N.D. Sung, K.S. Yun, Y.S. Park, J.G. Kim, I.H. Suh, Acta Crystallogr., Sect. C: Cryst. Struct. Commun. C57 (2001) 47;
(c) N.-D. Sung, K.-S. Yun, J.-G. Kim, I.-H. Suh, Acta Crystallogr., Sect. C: Cryst. Struct. Commun. C56 (2000) E370;
(d) M.J. Plater, M.R.S.J. Foreman, J.M.S. Skakle, J. Chem. Crystallogr. 30 (2000) 535;
(e) A.J. Blake, D.E. Hibbs, P. Hubberstey, C.E. Russell, Polyhedron 17 (1998) 3583.

[7] (a) Z. Xu, L.K. Thompson, C.J. Matthews, D.O. Miller, A.E. Goeta, C. Wilson, J.A.K. Howard, M. Ohba, H. Okawa, Dalton Trans. (2000) 69;

(b) S.S. Tandon, L.K. Thompson, M.E. Manuel, J.N. Bridson, Inorg. Chem. 33 (1994) 5555.

[8] (a) J.E. Andrew, A.B. Blake, J. Chem. Soc. A (1969) 1408;
(b) J.E. Andrew, P.W. Ball, A.B. Blake, Chem. Commun. (1969) 143;
(c) P.W. Ball, A.B. Blake, J. Chem. Soc. A (1969) 1415;
(d) P.W. Ball, A.B. Blake, J. Chem. Soc. Dalton Trans (1974) 852.

[9] (a) J.C. Dewan, L.K. Thompson, Can. J. Chem. 60 (1982) 121;
(b) M. Ghedini, G. De Munno, G. Denti, A.M.M. Lanfredi, A. Tiripicchio, Inorg. Chim. Acta 57 (1982) 87;
(c) P. Dapporto, G. De Munno, G. Bruno, M. Romeo, Acta Crystallogr., Sect. C: Cryst. Struct. Commun. 39 (1983) 718.

[10] (a) L.K. Thompson, S.K. Mandal, J.P. Charland, E.J. Gabe, Can. J. Chem. 66 (1988) 348;
(b) G. De Munno, G. Bruno, Acta Crystallogr., Sect. C: Cryst. Struct. Commun. C40 (1984) 2022;
(c) S.K. Mandal, L.K. Thompson, A.W. Hanson, J. Chem. Soc. Chem. Commun. (1985) 1709.

[11] L.K. Thompson, A.W. Hanson, B.S. Ramaswamy, Inorg. Chem. 23 (1984) 2459.

[12] (a) L.K. Thompson, F.L. Lee, E.J. Gabe, Inorg. Chem. 27 (1988) 39;
(b) G. De Munno, G. Denti, Acta Crystallogr., Sect. C: Cryst. Struct. Commun. C40 (1984) 616.

[13] L.K. Thompson, Can. J. Chem. 61 (1983) 579.

[14] L.K. Thompson, S.S. Tandon, Comm. Inorg. Chem. 18 (1996) 125.

[15] (a) C.L. Sheppard, S.S. Tandon, L.K. Thompson, J.N. Bridson, D.O. Miller, M. Handa, F. Lloret, Inorg. Chim. Acta 250 (1996) 227;
(b) L.K. Thompson, S.S. Tandon, M.E. Manuel, Inorg. Chem. 34 (1995) 2356;
(c) L.K. Thompson, S.K. Mandal, E.J. Gabe, F.L. Lee, A.W. Addison, Inorg. Chem. 26 (1987) 657.

[16] (a) L. Chen, L.K. Thompson, J.N. Bridson, Can. J. Chem. 71 (1993) 1086;
(b) L. Chen, L.K. Thompson, S.S. Tandon, J.N. Bridson, Inorg. Chem. 32 (1993) 4063;
(c) S.S. Tandon, L.K. Thompson, J.N. Bridson, Inorg. Chem. 32 (1993) 32;
(d) S.S. Tandon, L.K. Thompson, J.N. Bridson, M. Bubenik, Inorg. Chem. 32 (1993) 4621.

[17] P. Robichaud, L.K. Thompson, Inorg. Chim. Acta 85 (1984) 137.

[18] D. Attanasio, G. Dessy, V. Fares, Inorg. Chim. Acta 104 (1985) 99.

[19] B.S. Furniss, A.J. Hannaford, P.W.G. Smith, A.R. Tatchell, Vogel's Textbook of Practical Organic Chemistry, 5th ed., 1989, pp. 409.

[20] (a) G.M. Sheldrick, Methods Enzymol. 276 (1997) 628;
(b) G.M. Sheldrick, Acta Crystallogr., Sect. A (1990) 467.

[21] G.M. Sheldrick, T.R. Schneider, Methods Enzymol. 277 (1997) 319.

[22] A.J. Fry, R.G. Reed, J. Am. Chem. Soc. 91 (1969) 6448.

[23] (a) J.M. Scott, W.H. Jura, Can. J. Chem. 45 (1967) 2375;
(b) C.P. Andrieux, J.M. Saveant, J. Electroanal. Chem. 33 (1971) 453.

[24] M.S. Mubarak, D.G. Peters, J. Electroanal. Chem. 507 (2001) 110.

[25] (a) S.K. Talapatra, P. Chaudhuri, B. Talapatra, Heterocycles 14 (1980) 1279;
(b) M. Yoshifuji, R. Nagase, N. Inamoto, Bull. Chem. Soc. Jpn. 55 (1982) 873;
(c) R.G. Srivastava, P.S. Venkataramani, Synth. Commun. 18 (1988) 1537;
(d) R.S. Varma, R.K. Saini, O. Prakash, Tetrahedron Lett. 38 (1997) 2621;
(e) R.S. Varma, D. Kumar, J. Heterocycl. Chem. 35 (1998) 1539.

[26] J.W. Rogers, E.H. Sund, R.K. Hughlett, Tex. J. Sci. 43 (1991) 149.

[27] K. Nakamoto, Infrared and Raman Spectra of Inorganic and Coordination Compounds, 3rd ed., 1978, p. 448.

[28] G.B. Deacon, R.J. Phillips, Coord. Chem. Rev. 33 (1980) 227.